

NRL Memorandum Report 2206

AD718312

The Effect of Element Packing
on the Complete Radiation Patterns
of Arrays

R. J. BOBBER

Underwater Sound Reference Division

January 18, 1971



NATIONAL TECHNICAL
INFORMATION SERVICE

NAVAL RESEARCH LABORATORY
Underwater Sound Reference Division
P. O. Box 8337, Orlando, Fla. 32800

D D C
REF ID: A651150
FEB 22 1971

This document has been approved for public release and sale;
its distribution is unlimited.

23

Contents

Abstract	ii
Problem Status	ii
Problem Authorization	ii
Introduction	1
Technique	3
Spacing in a Circular Array	4
Spacing in a Square Array	5
Odd or Even	7
Square or Hexagonal Grid	8
Size	10
Equivalent Radius	10
General Nearfield-Farfield Relationships	12
Number of Maxima and Minima	13
Uniform Circular Piston	13
Infinite Strip	14
Magnitude of Maxima and Minima	16
Off Axis in the Near Field	17
Summary	17
Acknowledgment	18
References	18

Abstract

A limited study has been made to determine the optimum number, spacing, and configuration of point sources in arrays simulating circular and square continuous-plane radiators. The criteria for comparison of the directivity patterns of the array and the continuous radiator were specified as agreement of each lobe within 1 dB in level and 1° in location. Circular and square arrays of both odd and even numbers of point sources arranged in square and hexagonal configurations were investigated. An array was analyzed by reducing it to the equivalent shaded line in the plane of the pattern. A computer then was programmed to produce the pattern of the line. It was found that the pattern of an array of an even number of points arranged at the corners of squares of side 0.2λ simulates that of a plane piston within the prescribed limits, except within a half-wavelength of the array and in the region near 90° to either side of the principal axis.

Problem Status

This is an interim report on the problem; work is continuing.

Problem Authorization

NRL Problem S02-31

Project RF 05-111-401--4472

Manuscript submitted October 5, 1970.

THE EFFECT OF ELEMENT PACKING ON THE COMPLETE RADIATION PATTERNS OF ARRAYS

Introduction

An array of small transducers that approximate point sources often is used in underwater acoustics as a substitute for an extended continuous source. Large sonar transducers are constructed in this way as a matter of engineering feasibility. In theoretical work, an array of point sources provides a more manageable mathematical model than does a continuous plane or line radiator. In either case, it is desirable to use the minimum number of points that faithfully simulates a continuous source. Specifically, the question is: "How closely packed must be the point sources in an array to produce the same radiation pattern as a continuous-line or continuous-plane transducer?"

For many years, the rule of thumb in sonar transducer development has been that the packing interval or maximum point-to-point separation must be 0.8λ (0.8 wavelength). This rule was established during the pioneering sonar development of World War II [1]; apparently, it has proved to be a useful criterion.

A review of radiation theory shows that the spacing criterion 0.8λ is adequate only if interest is confined to the main lobe of the directivity pattern. To take a simple case for example, in Fig. 1, the directivity pattern level of a continuous line is compared with the patterns of lines of point sources at four angular directions from the acoustic axis. The angles were chosen to correspond approximately to the 10-dB-down levels of the major lobe and of the first, second, and third minor lobes in the pattern of a continuous line 3.2 wavelengths long. It is evident that near the axis ($\theta \leq 14^\circ$), or in the direction in which most of the acoustic power is radiated, the difference between the continuous line and a line of 4 points separated by 0.8λ is negligible. At greater angles, or in the minor lobe structure, however, the difference is considerable. Only with the spacing interval $d \leq 0.2\lambda$ are the entire patterns similar within 1 dB.

K. von Haselberg and J. Krautkrämer [2] have stated that "The requirements for freedom of the pattern from lobes and freedom from undulation in the near field seem to be identical." An extension of this thesis is that the number and relative magnitudes of the minor lobes in a far-field directivity pattern correspond to the number and relative magnitudes of the undulations in the near-field pressure distribution along the axis.

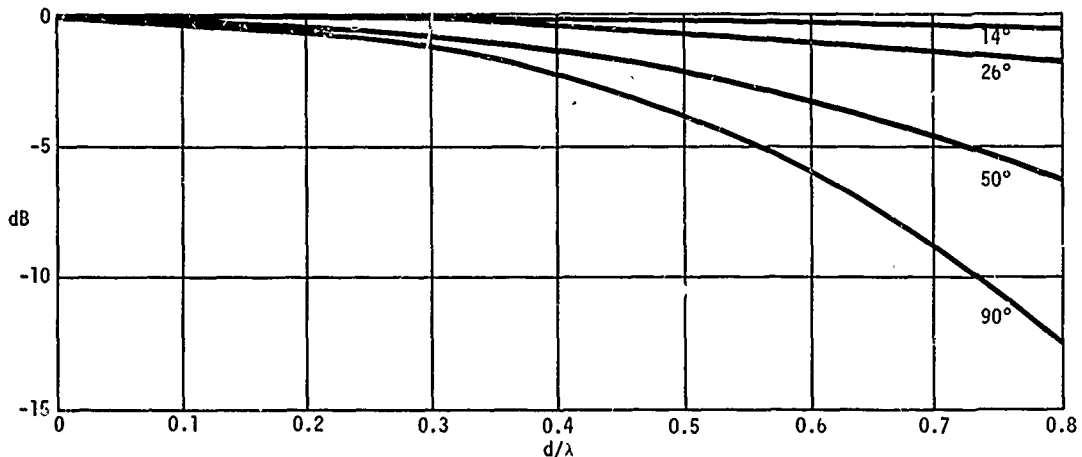


Fig. 1. Level of the pattern of a line of n point sources separated by distance d , relative to the level of the pattern of a uniform line of length $L = nd = 3.2\lambda$, where λ is the wavelength of sound in the medium; values shown for various angles from the axis.

If such is the case, then, the spacing criterion 0.8λ also is inadequate to produce near-field fidelity.

Because far-field patterns can be computed much more easily than can near-field patterns, it seemed worthwhile first to establish criteria for the effect of point spacing in an array on the minor-lobe structure of the far-field pattern; that is: "What is the maximum allowable point spacing for an array that must duplicate the complete far-field pattern of a plane source?" From Fig. 1, obviously, the spacing will be something less than 0.8λ . Once established, the spacing criterion for the far-field pattern can be assumed to apply to the near field as well. The correspondence between far-field-pattern minor lobes and near-field pressure undulations never has been mathematically proven, however, nor even empirically established. The assumption that such a correspondence holds now will be examined and tested for simple cases.

Trott [3] successfully used the von Haselberg-Krautkrämer concept in the design of his near-field array, and he found that the high-frequency limit of his array corresponded to the element spacing 0.8λ . This finding might seem, on first consideration, to be inconsistent with the implication of Fig. 1 that the spacing 0.8λ is inadequate. The Trott array, however, simulates a plane, nonuniform radiator specifically designed to eliminate minor lobes in the far-field pattern and undulations in the near-field axial pressure distribution. That is, the far-field pattern of the Trott array consists, essentially, only of the major lobe.

This report presents the results of an investigation on (1) the minor-lobe structure of the beam pattern of circular and square arrays as a function of spacing, configuration, odd or even number of point

sources, size of array, and the equivalent radius of an array that only approximates a circular piston; and (2) the relationship between minor lobes of the far-field pattern and the near-field undulations.

Technique

Several typical and practical arrays were designed with variations in spacing, arrangement, shape, and size. The computed directivity patterns then were compared with those of a circular or a square piston in a rigid baffle.

The criteria for good agreement between patterns were set at maximum differences of 1° between angles of minima and peaks, and 1 dB between levels, particularly the peak levels of minor lobes.

Initially, element separation of 0.8λ was assumed; then, the spacing was reduced to 0.5λ , 0.4λ , 0.3λ , and 0.2λ . Two basic configurations of elements were used: the square and the hexagonal. Arrangements of both odd and even numbers of elements were tried. The odd-numbered arrangement requires an element on the axis or at the center; the even-numbered arrangement requires a space in that position.

The first arrays were designed to fit inside a circle (or a square) of diameter (or side) 3.2λ , which is a typical size corresponding to a kD or wavenumber-diameter (or a side) product of 20 radians. Later, patterns of arrays of dimensions 1.6λ and 6.4λ were examined.

The array patterns were computed by reducing each array to an equivalent shaded line in the plane of the pattern. Figure 2 illustrates how each point source in the line is weighted according to the total source strength of the vertical slice of the array that the point on the line represents. The pattern of the shaded line then is computed.

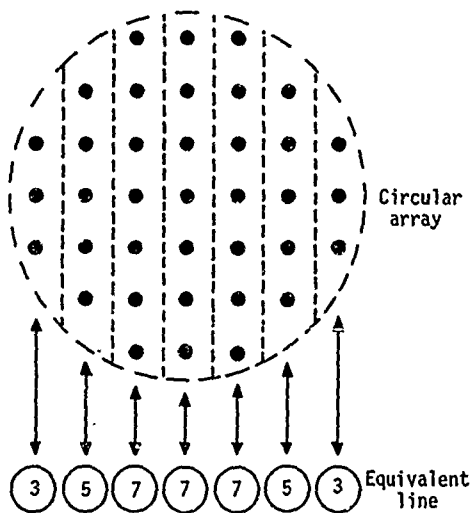


Fig. 2. A shaded line of point sources (below) having the same directivity pattern in the horizontal plane as the array of 37 uniform point sources (above). Each source in the line is weighted (shaded) in proportion to the number of sources in the corresponding vertical section of the array.

Spacing in a Circular Array

Starting with the point sources arranged in a square grid and spaced 0.8λ apart as shown in Fig. 3(a), the pattern of Fig. 3(b) was obtained. The array is a very coarse approximation to a circular piston. The pattern looks more like that of a line of four point sources, the third minor lobe being almost as high as the major lobe. (In the pattern of n uniform points, the level of the $(n - 1)^{\text{th}}$ minor lobe is the same as that of the major lobe.) Yet the major lobe still is a good approximation to that of the pattern of a piston of diameter 3.2λ . The pattern differences shown in Fig. 3 are of the same order of magnitude as those in Fig. 1.

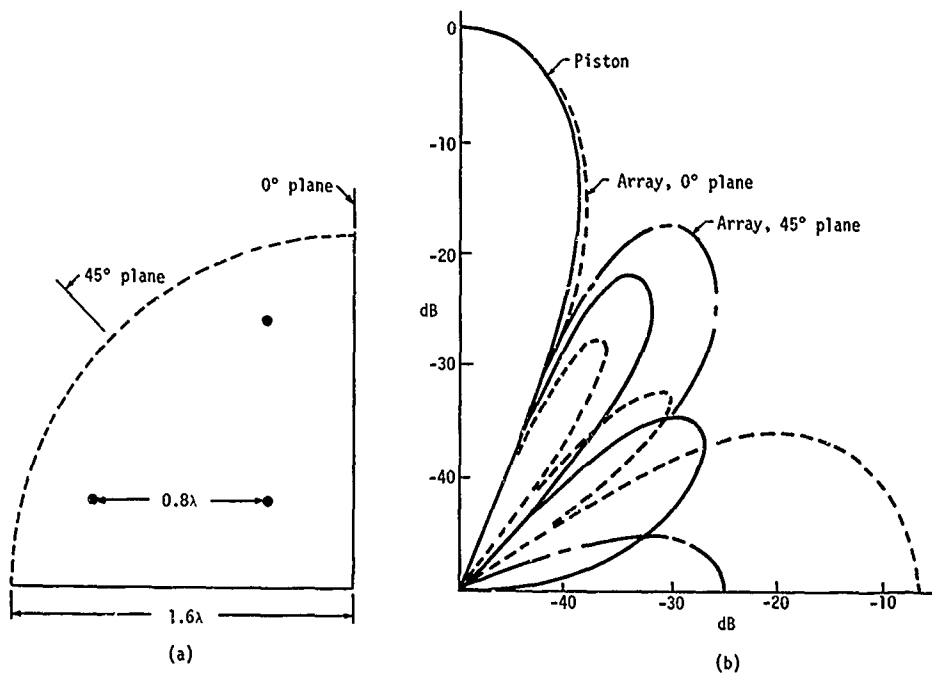


Fig. 3. (a) One quadrant of a circular array of an even number of point sources with 0.8λ square spacing. (b) Patterns of array in two planes, and of a uniform circular piston of radius 1.6λ .

When the spacing was reduced to 0.5λ , the patterns in the horizontal and the vertical planes approached those of a piston; still, there were differences of several dB between the levels of the minor-lobe peaks. The array continued to be a coarse approximation of a circular piston; the pattern symmetry to be expected from a circular piston was absent. Figure 4(b) shows the patterns in two planes of the array of Fig. 4(a).

Reducing the spacing to 0.4λ and then to 0.3λ gradually improved the agreement between piston and array patterns, but a maximum spacing of

0.2λ was required before the differences became less than 1° and 1 dB. Figure 5 shows the pattern for the spacing 0.2λ . The differences in Fig. 5(b) are barely discernible.

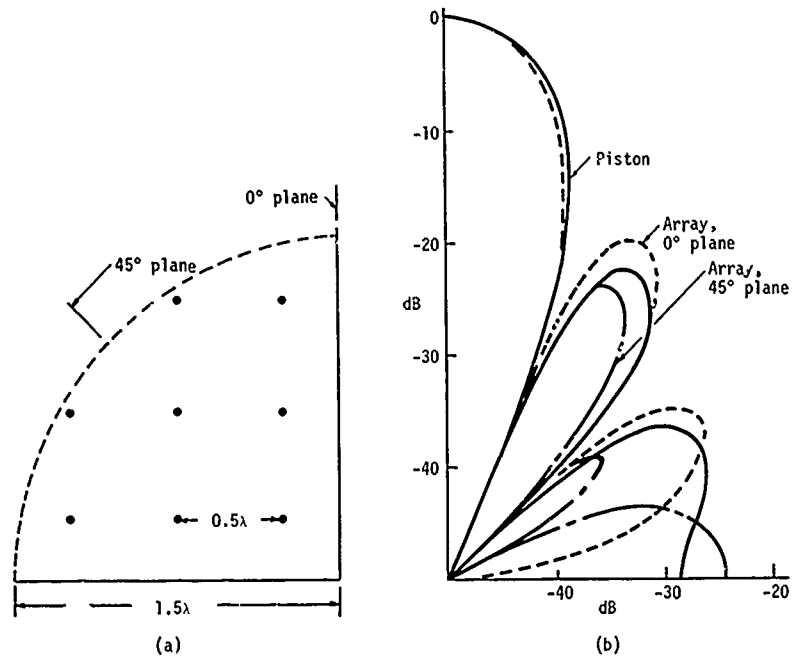


Fig. 4. (a) One quadrant of a circular array of an even number of point sources with 0.5λ square spacing. (b) Patterns of array in two planes, and of a uniform circular piston of radius 1.5λ .

Spacing in a Square Array

The spacing criterion for a square array was not found to be different from that for a circular array. The pattern in a plane normal to an edge and passing through the center of the square array is identical to that for a line of point sources; it is evident from Fig. 1 that the criterion 0.2λ applies.

When patterns were plotted for the plane normal to an edge for a square piston and for a square array with 0.2λ spacing, the differences were not discernible.

In a plane normal to the array through the diagonal of the square, the only noticeable difference was in a minor lobe some 40 dB down, as shown in Fig. 6.

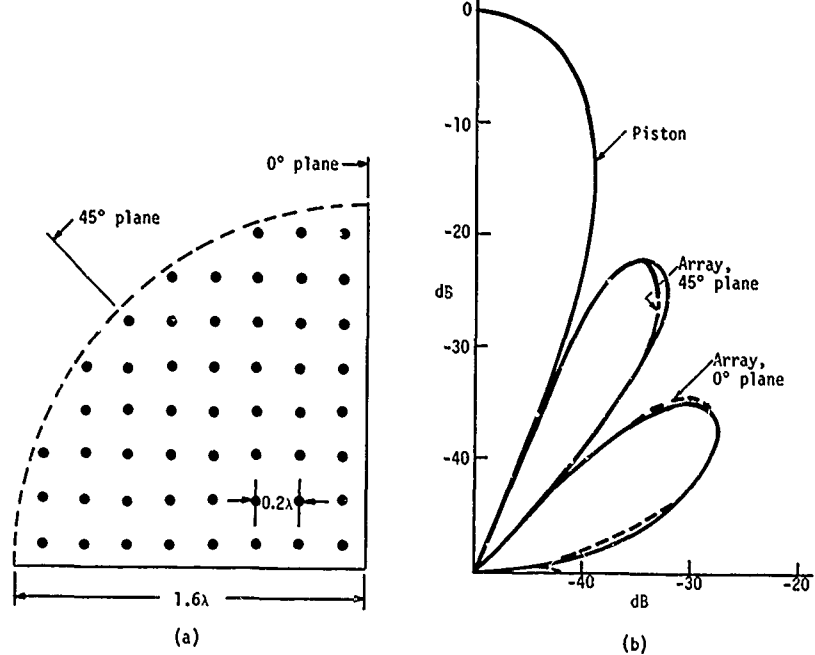


Fig. 5. (a) One quadrant of a circular array of an even number of point sources with 0.2λ square spacing. (b) Patterns of array in two planes, and of a uniform circular piston of radius 1.6λ .

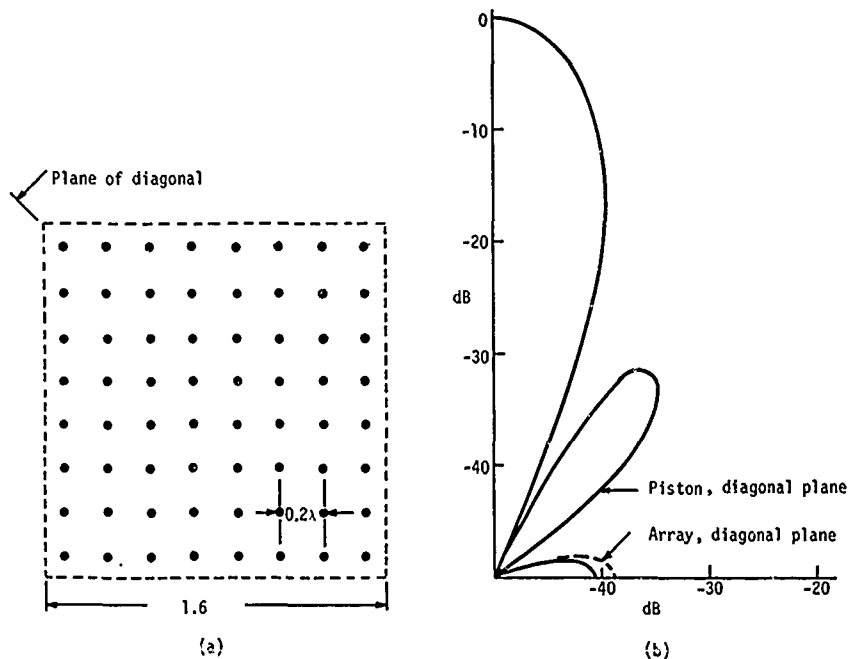


Fig. 6. (a) One quadrant of a square array of an even number of point sources with 0.2λ square spacing. (b) Patterns of array and of a uniform square piston 3.2λ wide, in the plane of the diagonal.

Odd or Even

If an array is designed with an element at its center and is otherwise symmetrical about the center, it must contain an odd number of elements. With a space at the center, it must contain an even number of elements. With a large number of elements, like, for example, the 208 in the entire array of Fig. 5, it would seem that whether the number be odd or even should make negligible difference; however, discernible differences were found.

Figure 7 shows the pattern for a circular array having an odd number of elements separated by 0.5λ compared with that for a piston of diameter 3.5λ . The differences in Fig. 7 are somewhat larger than the corresponding ones in Fig. 4.

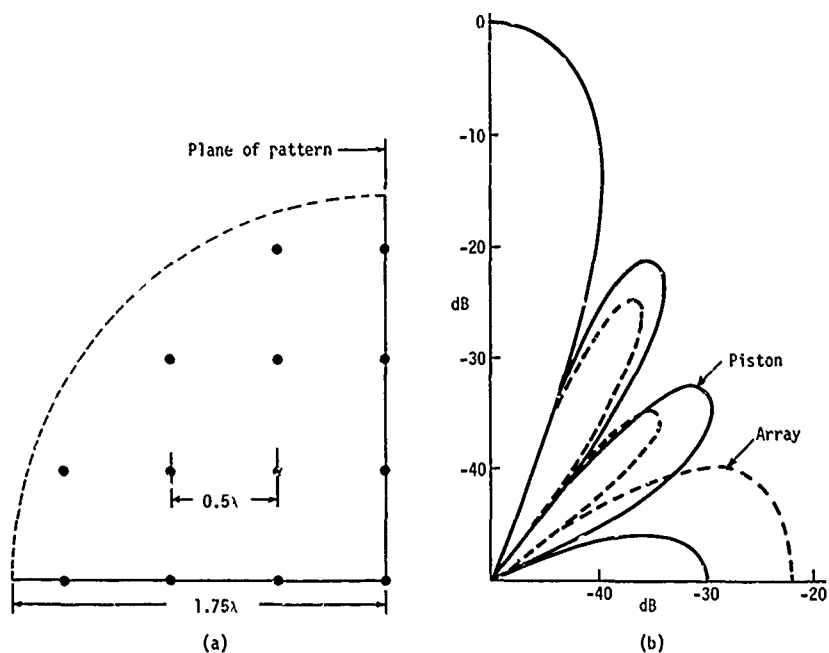


Fig. 7. (a) One quadrant of a circular array of an odd number of point sources with 0.5λ square spacing. (b) Pattern of array and of a uniform circular piston of radius 1.75λ .

When the separation is reduced to 0.2λ , the error in an "odd-array" pattern became smaller, but still was worse than that for an "even array." Figure 8 shows the patterns of an odd array with 0.2λ separation, and a piston of diameter 3.4λ . (The equivalent piston diameter was taken, in all cases, as the product of the element separation and the number of elements in the array diameter. For example, the array in Fig. 5 was taken as equivalent to a piston of diameter $16 \times 0.2\lambda = 3.2\lambda$.) The differences shown in Fig. 8b are slightly greater than those in Fig. 5.

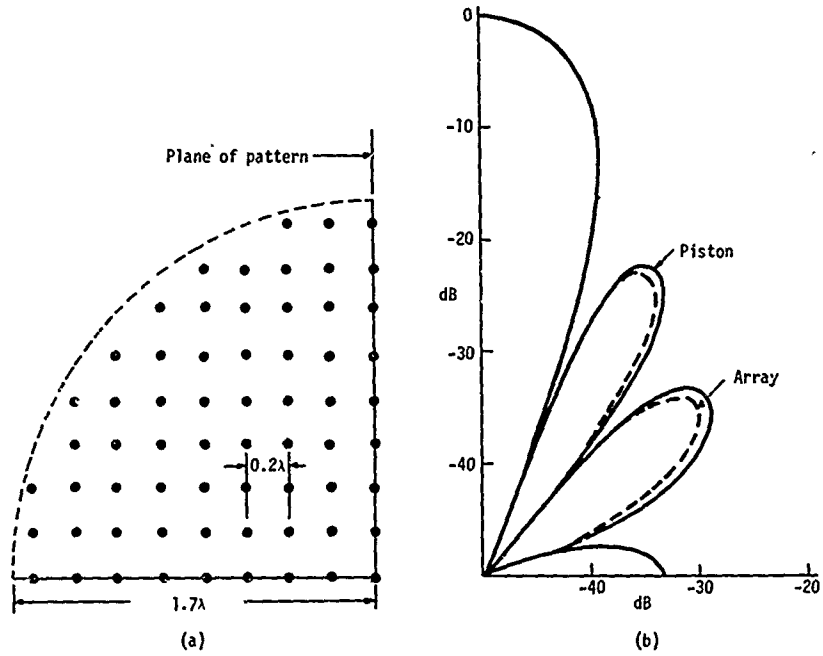


Fig. 8. (a) One quadrant of a circular array of an odd number of point sources with 0.2λ square spacing. (b) Pattern of array and of a uniform circular piston of radius 1.7λ .

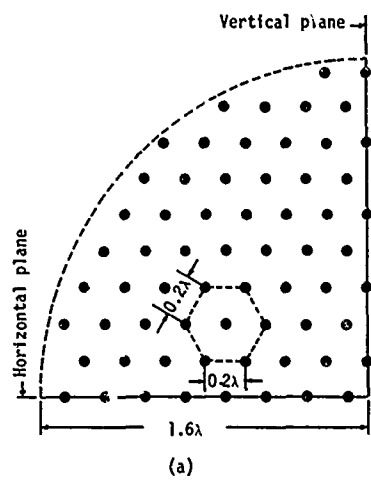
Figures 9 and 10, discussed in the next section, also show that an "even array" gives better results than an "odd array."

For circular arrays, the evidence is slightly in favor of even over odd; for square arrays, no significant difference was found between odd and even arrangements.

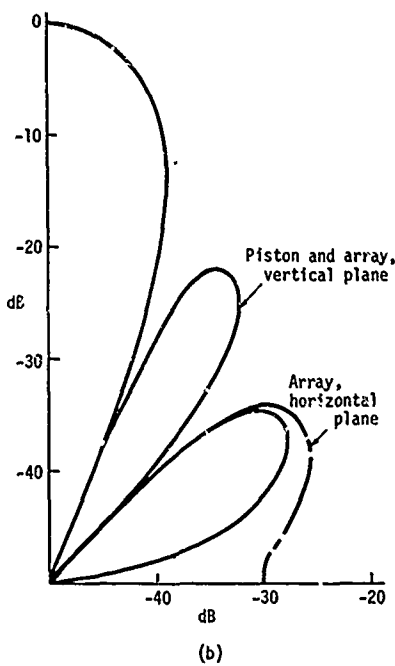
Square or Hexagonal Grid

Two basic grid configurations were used--the square grid shown in Figs. 3 through 8 and the hexagonal grid shown in Figs. 9a and 10a. In a real transducer array, the square grid is used if the individual elements are square; the hexagonal, if the elements are circular. Each case corresponds in practice to the closest and most logical packing arrangement of the two common shapes of elements. For the purpose of a mathematical model, the square grid fits into a rectangular coordinate system more easily than does the hexagonal grid. The square grid is more common and more convenient; the hexagonal grid provides closer packing of the elements or point sources.

Patterns of arrays with hexagonal grids are shown in Figs. 9b and 10b for 0.2λ spacing, even and odd arrangements, and two planes. Again, the symmetry of the pattern was best for the even array. In spite of the

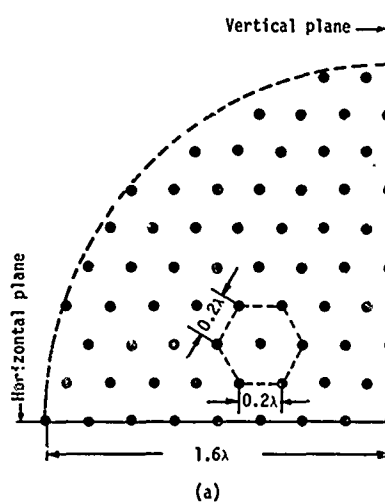


(a)

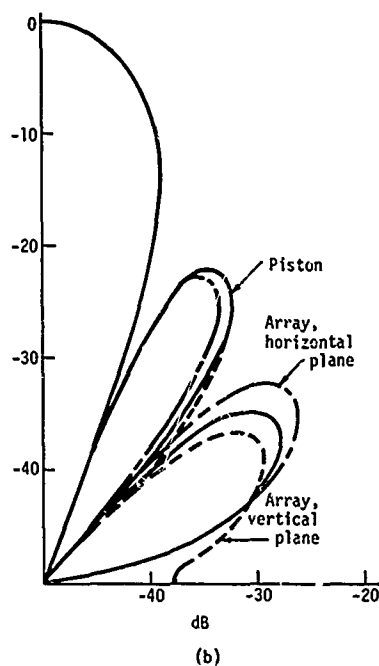


(b)

Fig. 9. (a) One quadrant of a circular array of an even number of point sources with 0.2λ hexagonal spacing. (b) Patterns of array in two planes, and of a uniform circular piston of radius 1.6λ .



(a)



(b)

Fig. 10. (a) One quadrant of a circular array of an odd number of point sources with 0.2λ hexagonal spacing. (b) Patterns of array in two planes, and of a uniform circular piston of radius 1.6λ .

fact that 0.2λ spacing constitutes closer packing in the hexagonal than in the square configuration, the agreement with the pattern of a piston source was poorer for the former (Figs. 9 and 10) than for the latter (Figs. 5 and 8). All of the disagreement was at angles greater than 55° . Perhaps it was the somewhat arbitrary design of the square and the hexagonal grid arrangements that caused the square grid to appear better. From considerations of convenience, as well as from Figs. 5, 9, and 10, however, the square-grid arrangement is preferred.

Size

The question of whether the spacing should be proportional to the array size was examined next. The patterns of a circular array of diameter 6.4λ (twice the typical 3.2λ) computed for 0.2λ and 0.4λ spacing are shown in Figs. 11 and 12. The former retains the 0.2λ spacing of Fig. 5; the latter retains the radius-to-spacing ratio of Fig. 5. The pattern of the 0.2λ array agrees closely with that of a piston of diameter 6.4λ through the first four minor lobes, or to a polar angle of about 50° . In the fifth and sixth minor lobes, there are differences of about 2 dB. The 0.4λ array shows differences exceeding 1 dB beginning with the third minor lobe and increasing to about 10 dB at 90° .

Similarly, the patterns of a circular array of diameter 1.6λ (half the typical 3.2λ) were computed for spacing of 0.2λ and 0.1λ . Both agreed within 1 dB with the pattern of a 1.6λ -diameter piston.

The 0.2λ maximum spacing criterion appears to be applicable for arrays in the diameter range $1.6\lambda \leq D \leq 6.4\lambda$.

Equivalent Radius

In all of the foregoing discussion, the equivalent radius of an array has been taken to be $n_r d$, where n_r is the number of point sources along the radius in the plane of the pattern, and d is the distance between points. Similarly, for a square array, the width has been taken as $n_w d$, where n_w is the number of point sources in a line parallel to an edge. For the pattern of a square in a plane through the acoustic center and normal to an edge, the procedure is mathematically valid, because the pattern function of a square piston in a rigid baffle is

$$P_\theta = \frac{\sin [(\pi W/\lambda) \sin \theta]}{(\pi W/\lambda) \sin \theta}, \quad (1)$$

where W is the width and θ is the angle measured from the acoustic axis. The pattern of a line of uniform point sources is

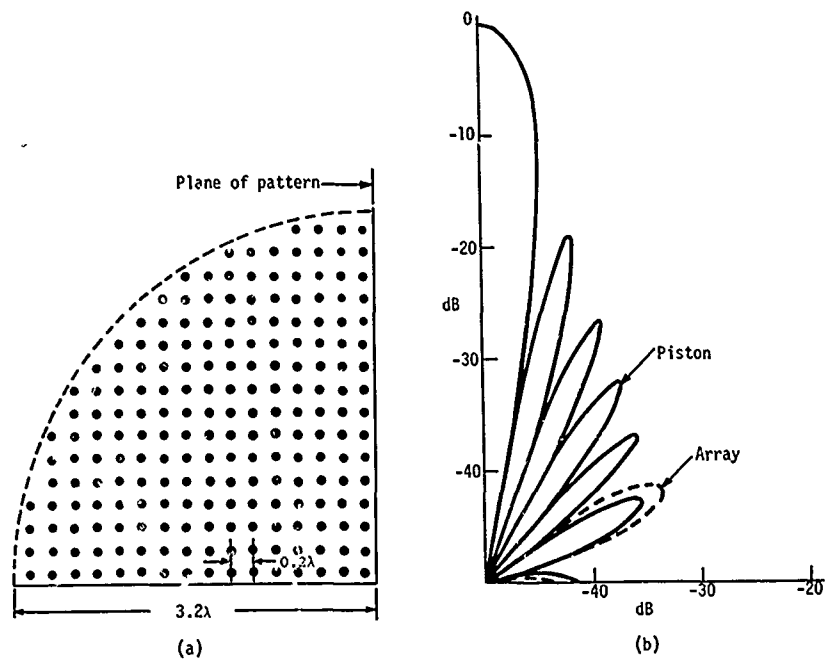


Fig. 11. (a) One quadrant of a circular array of an even number of point sources with 0.2λ square spacing. (b) Pattern of array, and of a uniform circular piston of radius 3.2λ .

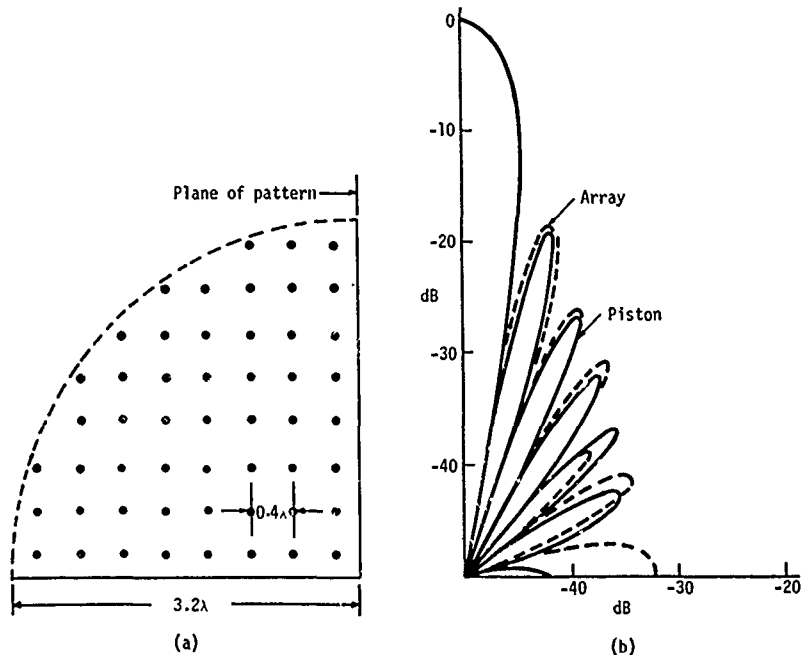


Fig. 12. (a) One quadrant of a circular array of an even number of point sources with 0.4λ square spacing. (b) Pattern of array, and of a uniform circular piston of radius 3.2λ .

$$P_\theta = \frac{\sin [(n_w d/\lambda) \sin \theta]}{n_w \sin [(\pi d/\lambda) \sin \theta]}. \quad (2)$$

The two patterns are the same when $n_w d = W$ and the small-angle approximation $\sin [(\pi d/\lambda) \sin \theta] \approx (\pi d/\lambda) \sin \theta$ can be used.

The case of a circular array is not so straightforward. The square-array equivalent of a square piston includes a uniform space of width $d/2$ beyond the outermost points. The circular-array equivalent of a circular piston includes beyond the outermost points a nonuniform space whose width varies from zero to $d/2$. (Compare Figs. 5a and 6a.) This situation arises, of course, because of the square spacing configuration in a circular array. Some points in a circular array actually can be at the circumferential outer limit. In Fig. 5a, for example, the outermost point nearest the 0° plane is approximately 1.5λ from the center. Other points are almost 1.6λ from the center. Because the equivalent radius should include the distance $d/2$, or 0.1λ in Fig. 5a, the equivalent radius should vary from 1.6λ to 1.7λ .

When the directivity patterns of the array in Fig. 5a were compared with the patterns of rigid pistons in an infinite baffle for radii of 1.6λ , 1.65λ , and 1.7λ , it was found that the equivalent radius actually varies from 1.6λ to 1.65λ ; however, the differences between the patterns of pistons of radii 1.6λ and 1.65λ are very small. The heights of the minor lobes are independent of the radius; therefore, they are the same for the two radii. The differences in angular position of the minima and maxima are less than 1° for angles less than 45° . The only large differences are found where the relative level is low (40 dB or more below the axial level).

Thus, an equivalent radius of $n_w d$ is acceptable, useful, and the best compromise between validity and simplicity.

General Nearfield-Farfield Relationships

The relation between the minor lobes of a far-field pattern and undulations in the near-field axial pressure distribution is difficult to describe precisely. "Undulations" and "lobes" are descriptive rather than quantitative terms or mathematical functions, yet the contention by von Haselberg and Krautkrämer [3] that the two are related is, no doubt, valid. From the work of Stenzel [4,5] one can visualize the generation and movement of pressure maxima in the near field of a piston transducer. As the frequency is increased, pressure maxima appear immediately in front of and at the center of the diaphragm. They then move both transversely outward from the center of the diaphragm and forward along the axis. The transversely moving maxima then appear as minor lobes at 90° and 270° in the far-field pattern. As the frequency continues to increase, the side lobes swing toward the axis, leaving room for more pressure maxima and new side lobes to follow.

A minimum can be identified more precisely than can a lobe or maximum, particularly if the minimum is a null. Consequently, nulls and minima, as well as lobes and maxima, were investigated.

Number of Maxima and Minima

To verify that the number of near-field axial pressure maxima or minima corresponds to the number of minor lobes or nulls in the far-field pattern, two radiator configurations were examined.

Uniform Circular Piston

Hueter and Bolt [6] give the positions of the maxima in the near-field pressure on the axis of a uniform circular piston as

$$y_{\max} = \frac{4R^2 - \lambda^2(2m + 1)^2}{4\lambda(2m + 1)}, \quad m = 1, 2, 3, \dots, m_1 \quad (3)$$

where the maximum for $m = 1$ is the most distant from the piston, and the one corresponding to m_1 occurs nearest the piston (that is, at $y = 0$). (NOTE: The term $m = 0$ in Hueter and Bolt corresponds to the maximum always present--even with an omnidirectional radiator; it corresponds to the main lobe of the pattern, and is not used here.)

The largest value of m --that is, m_1 , the total number of maxima--is found by setting $y_{\max} = 0$. See Fig. 13. Thus,

$$4R^2 - \lambda^2(2m_1 + 1)^2 = 0, \quad (4)$$

and

$$m_1 = (R/\lambda) - \frac{1}{2}. \quad (5)$$

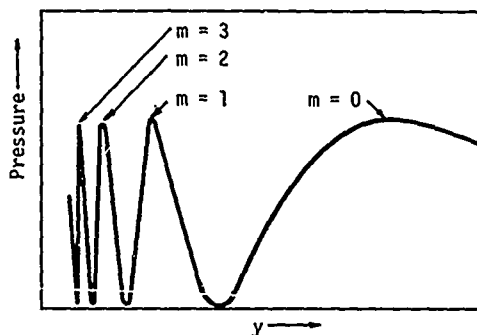


Fig. 13. Relative pressure in the near field on the axis of a circular piston.

Similarly, the positions of the axial minima are given by

$$y_{\min} = (R^2 - \lambda^2 m^2)/2m\lambda, \quad m = 1, 2, 3, \dots, m_2, \quad (6)$$

and the number of minima m_2 is given by

$$R^2 - \lambda^2 m_2^2 = 0,$$

or

$$m_2 = R/\lambda. \quad (7)$$

The directivity function p_θ of a uniform circular piston in a rigid baffle is

$$p = \frac{2J_1(kR \sin \theta)}{kR \sin \theta}. \quad (8)$$

This function is plotted in Fig. 14. The number of minor lobes from 0° to 90° is the same as the number of magnitude maxima in the range $0 \leq kR \sin \theta \leq kR$. The number of nulls in the pattern corresponds to the number of zero crossing points in the same range. From Fig. 14, one obtains Table 1, which can be used to deduce empirical rules for m_3 , the number of maxima or minor lobes in the directivity pattern, and m_4 , the number of zero points or nulls in the pattern:

$$m_3 = \frac{kR - 4}{3} = \frac{2\pi R}{3\lambda} \approx \frac{4}{3} \frac{R}{\lambda} \approx 2 \frac{R}{\lambda}, \quad (9)$$

$$m_4 = \frac{kR - 1}{3} = \frac{2\pi R}{3\lambda} \approx \frac{1}{3} \frac{R}{\lambda} \approx 2 \frac{R}{\lambda}. \quad (10)$$

Comparing Eqs. (9) and (10) with Eqs. (5) and (7) shows that $m_3 = 2m_1$ and $m_4 = 2m_2$. Thus, the number of pressure maxima and minima on the axis in the near field of a circular piston is one-half the number of minor lobes and nulls, respectively, in the far-field pattern between 0° and 90° . The approximations in Eqs. (9) and (10) are significant only when R/λ is small, or the pattern has only one minor lobe or one null.

Infinite Strip

Hueter and Bolt [6] give the position of the maxima in the near field and on the acoustic axis of an infinite strip as

$$y_{\max} = \frac{W^2 - (2m\lambda)^2}{8m\lambda}, \quad m = 1, 2, 3, \dots, m_5, \quad (11)$$

where W is the width of the strip. As before, the largest value of m , or m_5 , corresponds to $y_{\max} = 0$:

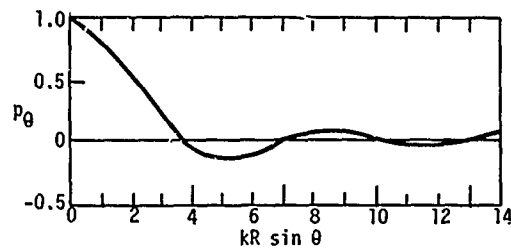


Fig. 14. Directivity function of a uniform circular piston of radius R , in a rigid baffle;
 $p_\theta = [2J_1(kR \sin \theta)]/(kR \sin \theta)$.

Table 1. Number of minor lobes and nulls in the directivity pattern of a uniform circular piston.

kR	(0 < kR sin θ \leq kR)	
	Lobes	Nulls
4	0	1
7	1	2
10	2	3
13	3	4

$$w^2 - (2m_5\lambda)^2 = 0,$$

and

$$m_5 = W/2\lambda. \quad (12)$$

Similarly, the positions of the minima are given by

$$y_{\min} = \frac{w^2 - (2m - 1)^2\lambda^2}{4m\lambda}, \quad m = 1, 2, 3, \dots, m_6.* \quad (13)$$

The largest value of m , or m_6 , is found by letting

$$w^2 - (2m_6 - 1)^2\lambda^2 = 0,$$

or

$$m_6 = (W/2\lambda) + \frac{1}{2}. \quad (14)$$

*NOTE: Hueter and Bolt's Eq. 3.15b incorrectly shows $m = 1, 3, 5, \dots$. The correct values are $m = 1, 2, 3, \dots$.

The theoretical far-field pattern of an infinite strip in the plane normal to the length is the same as that of a uniform line:

$$p = \frac{\sin [(\pi W/\lambda) \sin \theta]}{(\pi W/\lambda) \sin \theta}. \quad (15)$$

For values $0 < \theta \leq 90^\circ$, the zero crossing points (nulls) and maxima (lobes) can be determined by setting $\theta = 90^\circ$ and varying $W/2\lambda$. For example, the first null appears at 90° when $W/2\lambda = 0.5$, the second null when $W/2\lambda = 1.0$, and so on. The number of minor lobes m_7 , is one greater than m_8 , the number of nulls, thus:

$$m_7 = (W/\lambda) + 1 \quad (16)$$

$$m_8 = W/\lambda. \quad (17)$$

Equations (16) and (17) yield numbers twice as large as do Eqs. (14) and (12), respectively; however, in this case, the number of minor lobes is twice the number of near-field axial minima (rather than axial maxima, as in the case of the circular piston). Similarly, the number of nulls is twice the number of axial maxima.

It can be concluded, then, that the number of maxima (lobes) and minima (nulls) in the far field is proportional to the number of maxima and minima on the axis in the near field.

Magnitude of Maxima and Minima

The relative magnitude of the axial near-field pressure was computed as a function of array element spacing; some of the data are shown in Fig. 15. It was found that the axial pressure of an array with 0.2λ spacing was essentially identical to that of a plane piston, except at axial distances less than 0.1λ . For array spacing up to 0.5λ , the pressure maxima were within ± 1 dB of those for a piston, except at axial distances less than 0.5λ . Figure 15 shows again that the element separation 0.8λ gives poor simulation fidelity.

When the patterns in Figs. 3, 4, and 5 are compared with the curves in Fig. 15, there appears to be a correspondence between the pattern angle and the axial distance y/λ . That is, variations in the very-near field of an array appear to correspond to variations in the far-field pattern at angles near 90° and 270° . Obviously, differences between the near fields of a piston and of an array will be largest near the array. One would expect that, in the plane of the array ($y/\lambda = 0$), the two never could be identical. The implication, then, is that the patterns of arrays will differ from the patterns of pistons mainly at and near 90° and 270° .

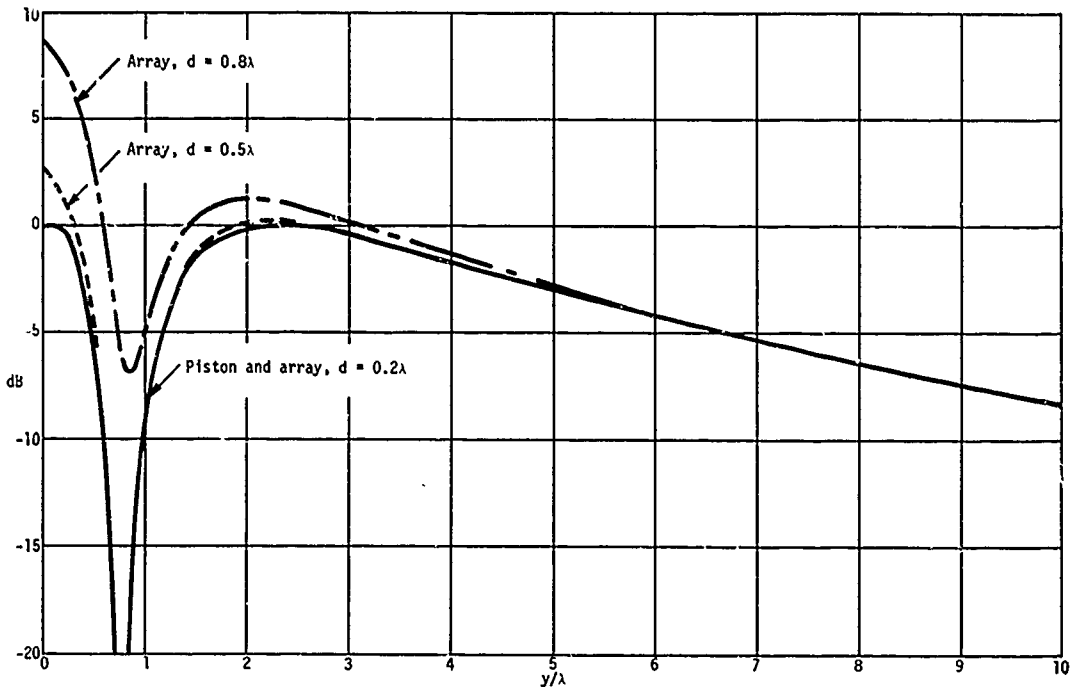


Fig. 15. Relative sound pressures on the axis of a circular piston and an array, as a function of the distance y from the plane of the source. Radius of piston or array is 1.6λ ; array element spacing is d .

Off Axis in the Near Field

The near sound field on the axis of a piston radiator is well known, and previous sections of this report have dealt with it. The sound pressure at the surface of a plane piston ($y/\lambda = 0$) also is well known, but (as already noted) this is the plane of maximum difference between the near fields of pistons and arrays. This leaves unexamined that part of the near field that is off the axis and away from the source. Stenzel [4] is the only author to provide any quantitative information on this subject; he presents the off-axis near field in the form of relatively imprecise contour plots. A comparison of the computed near field of an array with Stenzel's plots is too inconclusive to be useful. Because the axis of a circular radiator is the locus of points of maximum interference, extending our study to off-axis points in the near field would be of little purpose and much labor.

Summary

The objective here has been to ascertain how closely packed must be the elements in an array to simulate the radiation from a baffled plane

piston. The radiation field included the near field and the minor lobes in the far-field pattern. Emphasis was on circular radiators.

It was found that the pattern of an array with the element separation 0.2λ , a square packing arrangement, and an even number of elements would simulate, within ± 1 dB, that of a plane, infinitely baffled piston, except within a half-wavelength of the array and near 90° and 270° in the far-field pattern.

A secondary finding was that the number of minor lobes is twice the number of near-field axial maxima or minima.

Acknowledgment

The author is indebted to T. A. Henriquez and G. A. Sabin for programming the pattern computations.

References

1. *Design and Construction of Crystal Transducers*. Summary Technical Report of the National Defense Research Committee, Division 6, Vol. 12 (Washington, D. C., 1946), pp. 136-137 [AD-200 790; PB-139 777].
2. K. von Haselberg and J. Krautkrämer, "Ein Ultraschall-Strahler für die Werkstoffprüfung mit verbessertem Nahfeld," *Acustica* 9, 359-364 (1959).
3. W. J. Trott, "Underwater Sound Transducer Calibration from Nearfield Data," *J. Acoust. Soc. Amer.* 36, 1557-1568 (1964).
4. H. Stenzel, *Leitfaden zur Berechnung von Schallvorgängen* (Julius Springer, Berlin, 1939). See also NRL Translation No. 130.
5. H. Stenzel, "Die akustische Strahlung der rechteckigen Kolbenmembran," *Acustica* 2, 263-281 (1952).
6. T. F. Hueter and R. H. Bolt, *Sonics* (John Wiley & Sons, Inc., New York, 1955), Section 3.4.

UNCLASSIFIED

Security Classification

DOCUMENT CONTROL DATA - R & D

(Security classification of the body of abstract and indexing annotation must be entered when the overall report is classified)

1 ORIGINATING ACTIVITY (Corporate author)		2a. REPORT SECURITY CLASSIFICATION
Naval Research Laboratory Underwater Sound Reference Division P. O. Box 8337, Orlando, Florida 32806		Unclassified
2b. GROUP		
3 REPORT TITLE		
THE EFFECT OF ELEMENT PACKING ON THE COMPLETE RADIATION PATTERNS OF ARRAYS		
4 DESCRIPTIVE NOTES (Type of report and inclusive dates) An interim report on the problem		
5 AUTHOR(S) (First name, middle initial, last name) R. J. Bobber		
6 REPORT DATE January 18, 1971		7a. TOTAL NO. OF PAGES ii + 20
8a. CONTRACT OR GRANT NO NRL Problem S02-30		9a. ORIGINATOR'S REPORT NUMBER(S) NRL Memorandum Report 2206
b. PROJECT NO RF 05-111-401-4471		9b. OTHER REPORT NO(S) (Any other numbers that may be assigned this report)
c.		
d.		
10 DISTRIBUTION STATEMENT This document has been approved for public release and sale; its distribution is unlimited.		
11 SUPPLEMENTARY NOTES <i>1/12</i>		12 SPONSORING MILITARY ACTIVITY Department of the Navy (Office of Naval Research) Arlington, Va. 22217
13 ABSTRACT A limited study has been made to determine the optimum number, spacing, and configuration of point sources in arrays simulating circular and square continuous-plane radiators. The criteria for comparison of the directivity patterns of the array and the continuous radiator were specified as agreement of each lobe within 1 dB in level and 1° in location. Circular and square arrays of both odd and even numbers of point sources arranged in square and hexagonal configurations were investigated. An array was analyzed by reducing it to the equivalent shaded line in the plane of the pattern. A computer then was programmed to produce the pattern of the line. It was found that the pattern of an array of an even number of points arranged at the corners of squares of side 0.2λ simulates that of a plane piston within the prescribed limits, except within a half-wavelength of the array and in the region near 90° to either side of the principal axis. <i>→ half-wavelength</i>		

DD FORM 1 NOV 65 1473

S/N 0102-014-6600

(PAGE 1)

19

UNCLASSIFIED

Security Classification

UNCLASSIFIED
Security Classification

14. KEY WORDS	LINK A		LINK B		LINK C	
	ROLE	WT	ROLE	WT	ROLE	WT
Transducers - Arrays - Design Directivity patterns Point sources						